Atmospheric Environment 202 (2019) 167–179

Contents lists available at ScienceDirect

Atmospheric Environment

journal homepage: www.elsevier.com/locate/atmosenv

Improving ozone simulations in the Great Lakes Region: The role of emissions, chemistry, and dry deposition

Momei Qin[a], Haofei Yu[a,b], Yongtao Hu[a], Armistead G. Russell[a], M Talat Odman[a,*], Kevin Doty[c], Arastoo Pour-Biazar[c], Richard T. McNider[d], Eladio Knipping[e]

[a] School of Civil and Environmental Engineering, Georgia Institute of Technology, Atlanta, GA, USA
[b] Now at Department of Civil, Environmental and Construction Engineering, University of Central Florida, Orlando, FL, US
[c] Earth System Science Center, University of Alabama in Huntsville, Huntsville, AL, USA
[d] Department of Atmospheric Science, University of Alabama in Huntsville, Huntsville, AL, USA
[e] Electric Power Research Institute, Washington, DC, USA

ARTICLE INFO

Keywords:
CMAQ
Ozone
The great lakes region
CB6
MEGAN
NO_x emissions

ABSTRACT

The Great Lakes Region of the US continues experiencing exceedances of the ozone (O_3) standards, despite years of emissions controls. In part, this is due to interactions between emissions from surrounding large cities (e.g., Chicago) and meteorology, which is heavily influenced by the presence of the Great Lakes. These complex meteorology-emissions interactions pose a challenge to fully capture O_3 dynamics, particularly near shores of the lakes, where high O_3 levels are often experienced. In a simulation with the Community Multiscale Air Quality (CMAQ) model, using inputs as typically constructed, the model tends to be biased high. A literature review indicated that NO_x emissions from mobile sources, possibly overestimated in the 2011 National Emission Inventory (NEI), or the version of the Carbon Bond chemical mechanism used in CMAQ could be responsible for high biases of O_3. As such, a series of sensitivity tests was conducted to identify potential causes for this bias, including emissions biases (e.g., biogenic VOCs, anthropogenic NO_x), chemical mechanism choice, and O_3 dry deposition to fresh water, for high O_3 periods in July 2011. The base model/emissions configuration used the following: Carbon Bond mechanism CB05, biogenic emissions using Biogenic Emission Inventory System (BEIS), and anthropogenic emissions from the 2011 National Emissions Inventory (NEI). Meteorological inputs were developed using the Weather Research and Forecasting (WRF) model (version 3.8.1). Simulated daily maximum 8-h average O_3 without and with a cutoff of 60 ppb (referred to as MDA8 O_3 and elevated MDA8 O_3 hereafter, respectively) were evaluated against measurements. The evaluation showed a high bias in MDA8 O_3 across the domain, particularly at coastal sites (by ~6 ppb), while elevated MDA8 O_3 (i.e., greater than 60 ppb) was biased low, with exceptions centered along the shore of Lake Michigan. Using the CB6 chemical mechanism or 50% reduction of NO_x emissions from on-road mobile sources led to substantial domain-wide decreases in O_3 from the base case, and the model performance improved, particularly along the Lake Michigan shoreline and for the western domain. However, elevated MDA8 O_3 was more biased against measurements, compared to the model performance in the base case, except at a few sites along the shoreline. Using the Model of Emissions of Gases and Aerosols from Nature (MEGAN) instead of BEIS to estimate biogenic emissions, or increasing dry deposition of O_3 to fresh water by a factor of ten (which is unrealistic), had minor impacts on simulated O_3 over land. But, combining MEGAN with CB6 resulted in improved elevated MDA8 O_3 simulation along the western coast of Lake Michigan. Finally, using CB6 combined with a 30% reduction of on-road mobile NO_x emissions and MEGAN led to the best performance. Two companion papers investigate how meteorological modeling can be improved. Together, the recommended modeling system could serve as a starting point for future O_3 modeling in the region.

* Corresponding author.
E-mail addresses: talat.odman@ce.gatech.edu, odman@gatech.edu (M.T. Odman).

https://doi.org/10.1016/j.atmosenv.2019.01.025
Received 5 July 2018; Received in revised form 30 December 2018; Accepted 5 January 2019
Available online 19 January 2019
1352-2310/

1. Introduction

Exceedance of the National Ambient Air Quality Standard (NAAQS) for ozone (O_3) has been of concern in the Great Lakes Region for many years (Foley et al., 2011). Several counties located in the Milwaukee–Chicago–Gary urban corridor along Lake Michigan, which are densely populated areas with a variety of emission sources, have been violating the 2008, 0.075 parts per million 8-h O_3 standard (US EPA, 2018). Those counties are in violation of the more stringent 8-h O_3 standard of 70 parts per billion (ppb) promulgated in 2015 (https://www.epa.gov/ozone-designations/additional-designations-2015-ozone-standards), and will likely remain in non-attainment status for the near future.

Ground-level O_3 is primarily formed via chemistry involving volatile organic compounds (VOCs) and oxides of nitrogen (NO_x) in the presence of sunlight (Seinfeld and Pandis, 2012). High-O_3 episodes in the Great Lakes Region during summer have been tied to land-lake circulations, which are driven by temperature contrasts between the land and water (Dye et al., 1995; Lennartson and Schwartz, 2002; Levy et al., 2010; Makar et al., 2010b; Sills et al., 2011; Wentworth et al., 2015). In the early morning, O_3 precursors emitted onshore are transported by land breezes to over the lake. As sunlight intensifies, O_3 forms via reactions of the precursors confined within a shallow layer above the water and, along with reduced deposition velocities over water and little or no titration from fresh NO_x emissions, reaches high levels (Cleary et al., 2015; Levy et al., 2010). Offshore, O_3-rich air is then advected inland by afternoon lake breezes. Larger-scale synoptic flows (e.g., southerly/southwesterly winds over Lake Michigan) can partly affect O_3 levels over the region as well (Dye et al., 1995; Foley et al., 2011; Levy et al., 2010; Makar et al., 2010b).

The relative importance of NO_x and VOC emissions can also vary by location. Based on the analysis of 1994–2003 LADCO Aircraft Project (LAP) data, O_3 formation over Lake Michigan changes from VOC-limited in the morning to NO_x-limited in the afternoon at low altitudes (below 200 m), while the air mass is NO_x-limited throughout the day and more photochemically aged above 200 m (Foley et al., 2011). Measurements in the Greater Toronto Area from 2000 to 2012 suggest that O_3 production on land has become more sensitive to VOC reactivity, and has not been significantly decreasing in response to reductions of precursors over the study period (Pugliese et al., 2014).

In the late 1990s, photochemical grid models (e.g., UAM-IV (Urban Airshed Model with Carbon Bond IV) and UAM-V (Urban Airshed Model with Variable Grid)) have been applied to simulate O_3 episodes during the 1991 Lake Michigan Ozone Study (LMOS) (Hanna et al., 1996). Daily maximum 1-hr O_3 levels were typically overestimated by UAM-IV (by 12% on average) and slightly underestimated by UAM-V (by 3%) which uses higher photolysis rates, with underestimation of O_3 precursors (VOCs and NO_x) by as much as a factor of two. A major issue with these simulations was that high observed O_3 at 200–500 km downwind were both underestimated by 30–40 ppb, possibly due to problems with the simulated vertical diffusivities or the large underestimation of precursors, especially in rural areas. Fast and Heilman (2003) simulated O_3 that compared well with the observations over the western Great Lakes region, with a domain-wide average bias of −1.3 ppb for daily maximum 1-hr value and 5.5 ppb for the minimum. It was found that O_3 over the lakes and around the lake shores is very sensitive to lake temperatures: changes of 5°C in temperature contributing to as much as 50 ppb changes in O_3 mixing ratios. Makar et al. (2010a) demonstrated that substantial improvements in model performance for O_3, e.g., daily 1-hr maximum surface O_3 biases decreasing from ~15 ppb to ~9 ppb, were achieved in AURAMS (A Unified Regional Air-quality Modeling System) model through careful choice of the method used to specify lateral and top boundary conditions from O_3 climatology. However, reduction of surface O_3 bias sometimes came at the expense of significant positive biases in O_3 concentrations in the free troposphere and upper troposphere. Compared to ferry and land-based O_3 measurements, the Community Multiscale Air Quality (CMAQ) model presented higher positive biases over the water of Lake Michigan than over the surrounding land, up to 16 ppb for offshore locations with an increasing trend to the eastern side of the lake (Cleary et al., 2015). The WRF-Chem (Weather Research and Forecasting Chemical) model underpredicted peak O_3 during high-O_3 episodes in the forecasting products in support of 2017 LMOS campaign, which occurred during May and June 2017 to address the high O_3 events in coastal communities surrounding Lake Michigan (Stanier et al., 2017). Such efforts demonstrate that current chemical transport models have difficulties reproducing high-O_3 events due to unique meteorological and physical complexities associated with the area, along with general uncertainties concerning the emissions and chemistry (Simon et al., 2012).

In this study, the CMAQ model was used to simulate O_3 over the Great Lakes Region for July 2011. A series of sensitivity runs with different emissions, chemical mechanisms and/or O_3 dry deposition was conducted to identify model configurations and inputs best capturing land-based measurements. Improving O_3 modeling from meteorological perspectives (e.g., examining the roles of mixing and lake temperatures, or utilizing iterative WRF analysis) has been thoroughly explored in two companion papers (McNider et al., 2018; Odman et al., 2019b). This work focuses on the impacts of emissions, chemistry, and deposition, and aims to optimize CMAQ's O_3 performance over the Great Lakes Region.

2. Method

The CMAQ model (Byun and Schere, 2006) was applied to simulate O_3 in the Great Lakes Region during July 2011, driven by the Weather Research and Forecasting (WRF) model (Skamarock et al., 2005). July was selected as the study period because (1) it has the highest MDA8 O_3 concentration over the period of April to October and (2) simulated O_3 is more biased compared to measurements around Lake Michigan, based on our previous work (Odman et al., 2019a). Each model has a 4-km horizontal resolution domain nested inside a 12-km resolution domain. Initial conditions (ICs) and lateral boundary conditions (LBCs) for the outer domain ($12 \times 12\ km^2$ grid resolution) simulation were taken from the predefined CMAQ profiles, which represent relatively clean air conditions in the eastern-half of the United States (Gipson, 1999), while LBCs for the inner domain ($4 \times 4\ km^2$ grid resolution) simulation were obtained from the outer domain. The outer domain covers the entire contiguous US as well as a portion of Canada, while the inner domain focuses on the area surrounding the lakes (Fig. 1). In the vertical direction, there are 35 layers for both domains and the model top is placed at 50 hPa.

Fig. 1. Modeling domains of WRF (red boxes) and CMAQ (black boxes). A 4-km grid over the Great Lakes Region is nested inside a 12-km grid over the contiguous US. (For interpretation of the references to color in this figure legend, the reader is referred to the Web version of this article.)

2.1. Meteorological simulation

We used WRF version 3.8.1 to simulate the meteorological conditions. The analysis product of the North American Mesoscale Forecast System (NAM-12) provided initial and lateral boundary conditions for the simulation over the outer domain. The National Land Cover Database 2011 (NLCD2011) was used as land use/land cover data. The specific model configuration (Table S1) is the same as the initial iteration of iterative WRF analysis in Odman et al. (2019b). The simulation began on June 15th, and covered the entire month of July 2011. The first five days were used to initialize the deep soil moisture and temperature, as soil nudging was utilized to optimize surface temperature and humidity (Pleim and Gilliam, 2009; Pleim and Xiu, 2003). The rest of the simulation period used 5.5-day overlapping run segments, with the first 12 h included as the spin-up period.

2.2. Photochemical simulation

2.2.1. Base case

CMAQ version 5.1 with the latest version of Carbon Bond mechanism CB05, i.e., cb05e51, was applied to simulate the photochemistry taking place in the Great Lakes Region during the O_3 season. In this study, anthropogenic emissions are based on the US EPA 2011 National Emission Inventory (NEI). They were processed by the Sparse Matrix Operator Kernel Emissions (SMOKE) Modeling System following the EPA 2011v6.2 modeling platform (available at https://www.epa.gov/air-emissions-modeling/2011-version-62-platform). In-line plume rise calculations were carried out by CMAQ in this study. Additionally, biogenic emissions were calculated in-line with Biogenic Emission Inventory System (BEIS) version 3.6.1, which is imbedded in CMAQ as well. The simulation period spanned from June 20th to the end of July. We focused on the 4-km resolution inner domain to investigate model performance on simulating O_3 events throughout July 2011.

2.2.2. Sensitivity runs

Five sensitivity runs were conducted to explore the contributing factors to O_3 biases in the Great Lakes Region (Table 1). These runs were identical to the base case simulation in all respects, except for one or two factors (e.g., emissions, chemical mechanism or dry deposition of O_3) that were changed in the simulation over the inner domain for each case. Since we did not repeat the outer domain simulation with the modifications (except for the case with CB6), the ICs/LBCs for the inner domain would not reflect the change. Despite the uncertainties tied to unchanged boundary conditions, the sensitivity runs can still provide insight into the directionality and magnitude of the O_3 response. As such, the differences in simulated O_3 between a sensitivity run and the base case over the inner domain can still be attributed to the factor(s) that was (were) changed.

2.2.2.1. Biogenic emissions. Uncertainties in biogenic emissions were investigated by comparing two widely-used biogenic emission models. In the case labeled *Megan*, the Model of Emissions of Gases and Aerosols from Nature (MEGAN) version 2.1 (Guenther et al., 2012) was employed to estimate biogenic emissions, in place of BEIS used in the base case. The major differences between the two models include: (1) BEIS uses a leaf-scale emission factor at standard environmental conditions whereas MEGAN uses canopy-level emission factors, which are primarily based on leaf and branch-scale emission measurements that are extrapolated to the canopy-scale; (2) The built-in canopy models in MEGAN and BEIS are different, particularly in leaf temperature algorithms; (3) MEGAN accounts for the effect of leaf age and monthly changes of leaf area index (LAI), whereas BEIS does not (Bash et al., 2016; Pouliot and Pierce, 2009; Sindelarova et al., 2014).

MEGAN and BEIS were both driven by WRF, which provided meteorological fields such as temperature and radiation. In the base case with BEIS, BELD4 (Biogenic Emission Landuse Database) which contains gridded vegetation information for 275 vegetation categories, along with a normalized emission factor for each vegetation category, was provided as inputs to estimate emissions for 33 VOCs, CO, and nitric oxide (NO) (Bash et al., 2016). In the sensitivity run with MEGAN, the global gridded high-resolution emission potential map was utilized to estimate emissions of ten predominant compounds of biogenic origin (e.g., isoprene, monoterpenes, NO). This dataset was compiled based on species-specific emission factors and detailed vegetation species composition data (Guenther et al., 2012). Emissions of other compounds were estimated using plant functional type (PFT) and the PFT-specific emission factors. All the inputs including the gridded emission potential map, the PFT dataset and emission factors were provided together with MEGAN code except the LAIv (LAI of vegetation covered surfaces), which was retrieved from several MODIS (Moderate Resolution Imaging Spectroradiometer) satellite products as detailed in Yu et al. (2017).

2.2.2.2. NO_x emissions from mobile sources. 2011 NEI NO_x emissions, other than those from power plants, have been considered to be overestimated in multiple studies, with the magnitude of overestimation ranging from 14% to 70% (Anderson et al., 2014; Li et al., 2016; McDonald et al., 2018; Souri et al., 2016). Anderson et al. (2014) claimed high biases of NO_x emissions since higher ratios of CO/NO_x are measured in ambient air than that estimated by the 2011 NEI. However, the robustness of the basis of this claim has been questioned recently (Simon et al., 2018). Reductions of non-power-plant NO_x emissions decreased model biases for NO_x, inorganic nitrate and boundary layer ozone against aircraft measurements (Travis et al., 2016), and inverse modeling based on satellite NO_2 observations indicated a reduction in emissions from area (44%), mobile (30%), and point sources (60%) in high NO_x areas (Souri et al., 2016). Most importantly, projected NO_x emissions of mobile sources for 2013 using the 2011 NEI are 28% higher than the fuel-based inventory, with the largest discrepancies found in on-road gasoline sector (80% higher in the NEI), and the uncertainties in estimates of mobile emissions are associated with spatial and temporal patterns of activity, emission factors, and improved emission control technologies over time (McDonald et al., 2018 and references therein). Based on some of the above studies, mobile emissions that account for over half of NO_x emissions in the US, are most likely responsible for the high biases of NO_x emissions.

Considering that reducing mobile NO_x emissions could lead to better agreement with ambient measurements of NO_x or NO_y, as well as satellite retrievals of nitrogen dioxide (NO_2), and even better capture O_3 exceedances (Canty et al., 2015; Li et al., 2016; McDonald et al., 2018; Souri et al., 2016; Travis et al., 2016), a sensitivity run with a 50% reduction of NO_x emissions from on-road mobile sources, which are major contributors to mobile sources (the case *0.5NO$_x$*), was conducted to quantify the impact of a potential NO_x emission bias in the 2011 NEI on simulated O_3 in the Great Lakes Region.

2.2.2.3. Chemical mechanism. CB6, a newer version of Carbon Bond

Table 1
Summary of the base case and five sensitivity simulations.

NO.	Case	Biogenic emissions	On-road mobile NO_x emissions	Chemical mechanism	Dry deposition over fresh water
0	Base	BEIS	100%	CB05	Default
1	Megan	**MEGAN**	100%	CB05	Default
2	0.5NO_x	BEIS	**50%**	CB05	Default
3	CB6	BEIS	100%	**CB6**	Default
4	CB6_megan	**MEGAN**	100%	**CB6**	Default
5	Ddep	BEIS	100%	CB05	**10-fold**

Table 2
Model performance on daily maximum 8-h (MDA8) O_3 in the base and final simulations.

Site (No. of obs.)	Case	MB (ppb)	ME (ppb)	FB (%)	FE (%)	NMB (%)	NME (%)	MNB (%)	MNE (%)	RMSE (ppb)	IOA	r^2
Coastal (N = 1946)	Base	6.3	10.5	12.4	19.6	12.4	20.4	16.7	23.2	14.1	0.8	0.4
	Final	4.5	10.0	9.5	19.1	8.8	19.6	13.6	22.3	13.5	0.7	0.3
Buffer (N = 1559)	Base	1.8	7.1	4.7	14.0	3.5	13.9	6.8	15.4	9.4	0.8	0.5
	Final	0.0	7.3	1.5	14.6	0.0	14.3	3.6	15.4	9.5	0.8	0.4
Inland (N = 5113)	Base	2.4	7.5	5.1	14.0	4.4	13.8	7.4	15.6	9.8	0.8	0.4
	Final	0.1	7.4	1.0	14.1	0.1	13.7	3.1	15.1	9.7	0.8	0.4
All (N = 8618)	Base	3.2	8.1	6.6	15.3	6.0	15.3	9.4	17.3	10.9	0.8	0.4
	Final	1.1	8.0	3.0	15.3	2.0	15.1	5.6	16.8	10.6	0.8	0.4

chemical mechanism as an update to CB05, aims to better represent oxidant formation from long-lived, abundant VOCs, and the fate of organonitrates, particularly the recycling of NO_x (Yarwood et al., 2010). Some notable updates from CB05 to CB6 related to O_3 simulation include: (1) updated reactions of alkanes, alkenes and aromatics with the most changes for isoprene and aromatics; (2) long-lived VOCs, specifically propane, benzene, acetone and other ketones being explicitly represented; and (3) changed reaction rates, e.g., increasing the photolysis/OH oxidation rate of NO_2 by 5–7%, and decreasing the reaction rate of N_2O_5 with water vapor by ~80%. Several revisions have been made to CB6 (i.e., CB6r1, CB6r2, CB6r3 and CB6r4): for instance, CB6r1 revised the chemistry of isoprene and aromatics, and enhanced NO_x-recycling from the evolution of organonitrates (Yarwood et al., 2012); the fates of organonitrates were more detailed in CB6r2, with different partitioning into the condensed phase and dominant degradation pathway between simply the alkyl nitrates and the multi-functional organonitrates (Hildebrandt Ruiz and Yarwood, 2013); CB6r3 adopted temperature- and pressure-dependent NO_2-alkyl nitrate branching, which might improve O_3 simulation in winter (Stoeckenius and McNally, 2014). The third version of CB6 (CB6r3), which was recently implemented in CMAQv5.2, was used in the sensitivity run (the case *CB6*) in place of a revised version of CB05 (CB05e51) in the base run. While several reaction rates and product updates are present in both CB6r3 and CB05e51, CB6r3 has more comprehensive updates (Wyat Appel et al., 2018). Since CB6 is not available in CMAQv5.1, we switched to CMAQv5.2 for this simulation, which includes multiple updates that might lead to differences between the two runs collectively. Additionally, unlike other sensitivity runs, CB6 was applied to the outer domain as well as the inner domain for the case *CB6*.

CB05e51 in CMAQv5.1 has already incorporated detailed isoprene chemistry (Fahey et al., 2017) with some reaction rates and products from CB6r2, but there are slight differences in representation of isoprene chemistry between CB05e51 and CB6r3. For instance, CB6r3 considers the reaction of isoprene peroxy radical (ISO2) with other peroxy radicals (RO2), while CB05e51 does not; the fates of organonitrates via the reaction of isoprene with NO_3 radical are not the same, which affects the NO_x recycling efficiency. For this reason, the combined impact of CB6 with MEGAN emissions (the case *CB6_megan*) was also examined.

2.2.2.4. O_3 dry deposition over water. Dry deposition accounts for ~20% of O_3 removal from the troposphere (Lelieveld and Dentener, 2000). With dry deposition entirely turned off in the model, simulated surface O_3 increased by up to 50 ppb in the UK, particularly at night (Vieno et al., 2010). Underestimation of dry deposition with the Wesely scheme, based on Wesely (1989), can in part explain high biases of O_3 in the eastern US (Lin et al., 2008; Travis et al., 2016). The M3DRY scheme in the CMAQ model yields even lower dry deposition velocities than the Wesely scheme, which will result in higher O_3 concentrations, particularly when vegetation-dominated O_3 dry deposition over land is significant (Park et al., 2014). CMAQ v5.1 accounts for the interaction of O_3 with iodide in seawater, increasing deposition velocities by an order of magnitude and reducing summer-time surface O_3 concentration by ~3% over marine regions in the Northern Hemisphere (Sarwar et al., 2015). In this study, the dry deposition velocity of O_3 over the lakes was increased by a factor of 10, which is comparable to that over seawater in Sarwar et al. (2015), in order to investigate if potentially underestimated dry deposition rates over fresh water could be responsible for overestimation of O_3 over the lake and along the shoreline.

2.2.3. The final simulation

Based on the evaluation of modeled O_3 against ground-based measurements for each sensitivity run, the options for biogenic emission, adjusted NO_x emissions from on-road mobile sources and the chemical mechanism that had the best overall performance were used for the final simulations over the outer and inner domains, respectively.

2.3. Evaluation

Model performance was evaluated against the observed concentrations of ground-level O_3 and NO_x, which were obtained from the Air Quality System (AQS) network. The observations and simulations were paired in space and time. Monitoring sites located within the 4-km domain were considered for evaluation and were sorted into three groups based on the distance from the shoreline, i.e., coastal sites (< 20 km), sites in the buffer area (20–100 km), and inland sites (> 100 km), with 65, 52 and 174 sites, respectively, in each group. A variety of statistical metrics (Emery et al., 2017) including mean bias (MB), mean error (ME), fractional bias (FB), fractional error (FE), normalized mean bias (NMB), normalized mean error (NME), mean normalized bias (MNB), mean normalized error (MNE), index of agreement (IOA), coefficient of determination (r^2), and root mean squared error (RMSE) were used to evaluate daily maximum 8-hr average (MDA8) O_3, with or without a 60 ppb cutoff (Tables 2–3), and hourly NO_x.

3. Results and discussion

3.1. Base case simulation

Simulated ground-level MDA8 O_3 showed much higher concentrations over water than the surrounding land (Fig. 2 (a)), with the maximum exceeding 90 ppb over the southwestern side of Lake Michigan, corresponding to a land-lake contrast of ~30 ppb. Although no O_3 measurements over the lakes are available during July 2011, the simulated land-lake differences are greater than those reported in Levy et al. (2010) for ferry-based O_3 measurements over Lake Erie, which were 5–10 ppb above observations at rural sites nearby and 10–20 ppb larger than observations at urban sites in the southern Great Lakes Region. The daytime land-lake differences of O_3 were attributed to the lower dry deposition of O_3 to water than to land, which is true both for the real atmosphere and the model, and stable air over the lakes leads to conditions conducive to O_3 formation. A decreasing trend of simulated O_3 from the southern/central areas of Lake Michigan to the northern

Table 3
Model performance on elevated daily maximum 8-h (MDA8) O_3 (> 60 ppb) in the base and final simulations.

Site (No. of obs.)	Case	MB (ppb)	ME (ppb)	FB (%)	FE (%)	NMB (%)	NME (%)	MNB (%)	MNE (%)	RMSE (ppb)	IOA	r^2
Coastal (N = 555)	Base	0.0	10.0	−1.3	14.7	0.0	14.6	0.4	14.6	12.9	0.5	0.1
	Final	−2.9	10.7	−5.7	15.9	−4.3	15.6	−3.8	15.4	13.4	0.5	0.1
Buffer (N = 382)	Base	−5.6	8.2	−9.2	13.0	−8.3	12.2	−8.0	12.0	10.4	0.5	0.1
	Final	−8.7	10.1	−14.3	16.4	−12.9	15.1	−12.5	14.8	12.2	0.5	0.1
Inland (N = 1633)	Base	−2.8	7.5	−5.0	11.5	−4.2	11.2	−4.0	11.1	9.4	0.7	0.2
	Final	−5.7	8.8	−9.6	13.9	−8.5	13.0	−8.3	12.9	10.7	0.6	0.2
All (N = 2570)	Base	−2.6	8.2	−4.8	12.4	−3.9	12.1	−3.6	12.0	10.4	0.6	0.2
	Final	−5.6	9.4	−9.5	14.7	−8.3	13.9	−8.0	13.7	11.6	0.6	0.2

end was simulated. O_3 formation was enhanced over water near the Milwaukee–Chicago–Gary urban corridor, where a divergence zone was formed as a result of interaction of predominant westerly/southwesterly flow with lake breeze circulation; on the other hand, the air mass from the west is VOC limited, while the air from the east is NO_x limited, with the transition between these two air masses creating a mixture that is conducive to ozone production (Pour Biazar et al., 2018). Prevailing southwest winds transported O_3 northward before moving inland as described in Foley et al. (2011) and Hanna et al. (1996), contributing to moderate O_3 levels (MDA8 O_3 > 50 ppb) over the northern end of Lake Michigan.

Onshore observations at the AQS sites showed similar spatial variability of MDA8 O_3 with the simulation (Fig. 2 (b) (c)), with r^2 of 0.6 and elevated O_3 centered in the southern part of the domain. The observed concentrations along the shoreline of Lake Michigan and Lake Erie were mostly in the range of 50–60 ppb, and were lower along Lake Ontario and the northern end of Lake Michigan (40–50 ppb). By comparing with observations on land, it was found that CMAQ tended to overestimate MDA8 O_3 (although "elevated MDA8 O_3", i.e., MDA8 O_3 with a cutoff of 60 ppb, was specifically biased low), with the overestimation evident in locations where low to moderate O_3 occurred.

The diurnal trends of O_3 (red line in Fig. 3) indicated a high bias throughout the day, except for a few hours in the late afternoon (approximately 18:00–21:00 CST) when the observations were slightly higher. The overestimation of O_3 was most evident in the early morning (0:00–5:00 CST) and over the peak period of O_3 (8:00–16:00 CST). Biases in the morning could be a result of mixing in CMAQ as discussed by McNider et al. (2018), which is consistent with the insensitivity of the bias to perturbation of NO_x emissions in the sensitivity run *0.5NO$_x$*, suggesting that the morning bias might have less to do with chemistry than modeling system physics. McNider et al. (2018) noted that mixing in the stable boundary layer at this stage is highly uncertain (Bosveld et al., 2014) and may depend on vertical resolution, meaning that mixing might be a viable explanation. See also Savijärvi (2009). High biases for the peak concentrations were in part explained by uncertainties in NO_x emissions from mobile sources as the discrepancies decreased significantly in the case *0.5NO$_x$*, particularly at sites more than 20 km from the shoreline. While McNider et al. (2018) found evidence of excessive mixing in the NOAA NAM real-time forecast system, this actually introduced reduced mixing in CMAQ when mixing coefficients were re-diagnosed in CMAQ. Using the same PBL scheme in WRF and CMAQ in the present study should have minimized the error.

Elevated biases (positive) of the simulated MDA8 O_3 against the observations were concentrated around urban areas, e.g., Pittsburgh, Minneapolis, and along the shoreline of Lake Michigan (top row in Fig. 4) were over 10 ppb in most locations. Average simulated MDA8 O_3 for the coastal sites was 58 ppb, compared to 51 ppb in the observations (NMB of 12%, Table 2), while model-observation differences for buffer/inland areas were ~2 ppb (NMB of 4%). In contrast, MDA8 O_3 that was greater than 60 ppb in the observations (i.e., elevated MDA8 O_3), with a chance of ~30% occurrence during the simulation period (the number of days with observed MDA8 O_3 above 60 ppb at each site is shown in Fig. S1), exhibited domain-wide underestimation except for a few locations, e.g., along Lake Michigan where overestimates remained for elevated MDA8 O_3. For inland sites, the simulations were ~3 ppb lower than the observations (NMB of −4%, Table 3), while they were almost unbiased at coastal sites (NMB of −0%). Although no observations over the lakes are available for evaluation of simulated O_3 over water, higher biases of O_3 along the shoreline of Lake Michigan than elsewhere showed good agreement with biases over water in Cleary et al. (2015). As discussed in McNider et al. (2018), part of the over-prediction in Cleary et al. (2015) was due to re-diagnosed mixing coefficients in CMAQ.

Simulated NO_x was also compared with observations, as NO_x influences O_3 formation and destruction. NO_x emissions from mobile sources in 2011 NEI are deemed to be overestimated in several studies (Anderson et al., 2014; Li et al., 2016; McDonald et al., 2018; Souri et al., 2016), and our simulation supported this hypothesis. Overall NO_x in the simulation is ~2 ppb higher than the observations (Fig. 3). Observed NO_x remained high overnight and peaked around 6:00 CST, resulting from emission patterns as well as a shallow boundary layer over that period. Two peaks were observed in the simulation: one at about 5:00 CST and the other at 20:00 CST. The largest model-observation differences occurred at these times. The concurrency of maximum model-observation gap and rush hour traffic suggested that biases are related to overestimated emission inventory for vehicles. Another factor which may be relevant to the over-prediction of NO_x may be wind speed bias in the meteorological simulations. The WRF run for 2011 showed that surface wind speeds at night and in the morning were significantly higher than observed (McNider et al.,

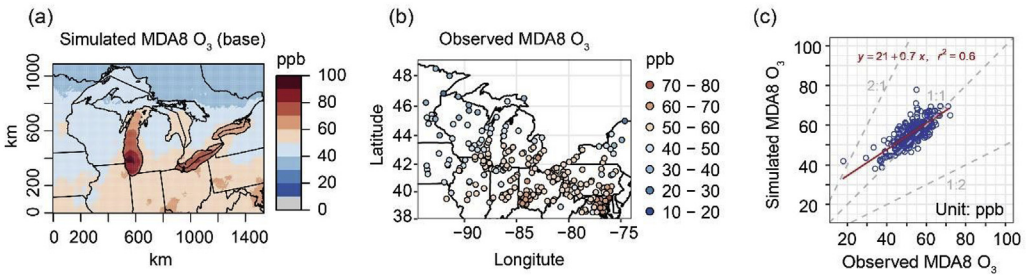

Fig. 2. July 2011 averages of (a) Simulated daily maximum 8-h (MDA8) O_3 in the base case, and (b) Observed MDA8 O_3 at the air quality system (AQS) sites in the Great Lakes Region. (c) Scatter plot of the simulations against observations at the AQS sites.

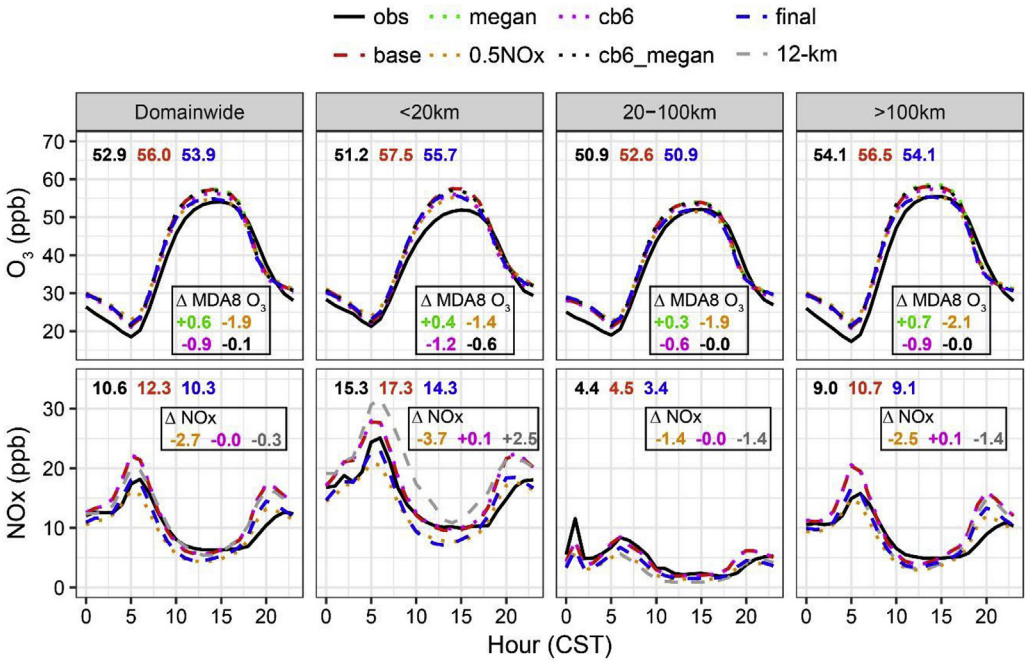

Fig. 3. Diurnal trends of O_3 (top) and NO_x (bottom) averaged across the domain (Domainwide), at coastal (< 20 km), buffer (20–100 km), and inland (> 100 km) sites in the Great Lakes Region in July 2011. Monthly means of MDA8 O_3 and NO_x from observations (black), simulations in the base (red) and final (blue) runs at the AQS sites are shown at the top of each panel. Changes in MDA8 O_3 and NO_x in each sensitivity run with respect to the base case are shown in the small boxes. (For interpretation of the references to color in this figure legend, the reader is referred to the Web version of this article.)

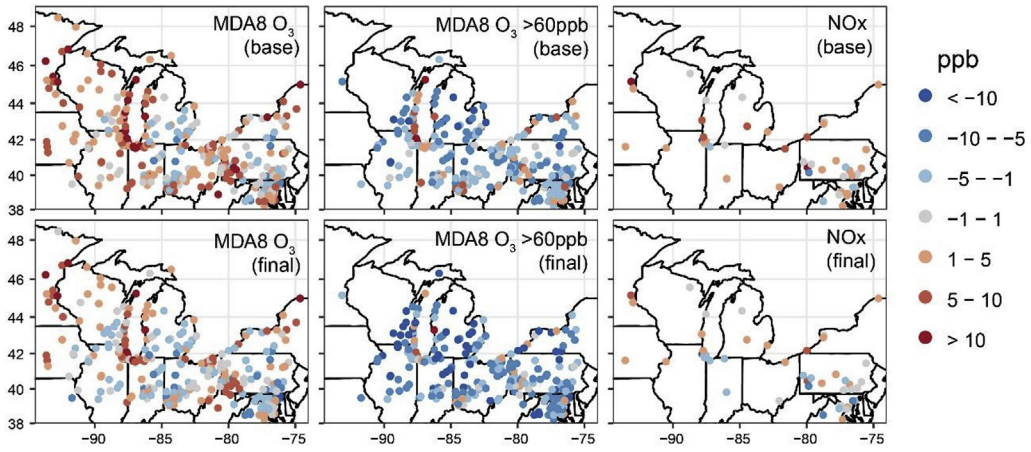

Fig. 4. Mean biases of simulated MDA8 O_3 (with/without a cutoff of 60 ppb) and NO_x concentrations from the base (top) and final (bottom) simulations against the observations in the Great Lakes Region in July 2011.

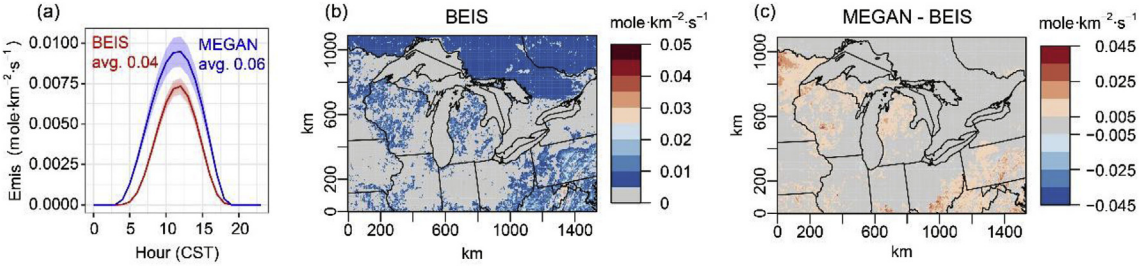

Fig. 5. (a) Diurnal trends of isoprene emission using BEIS and MEGAN with the daytime (6:00–18:00 CST) averages across the domain shown at the top of the panel. (b) Daytime isoprene emission using BEIS over the Great Lakes Region in July 2011. (c) Differences in isoprene emission between MEGAN and BEIS over the Great Lakes Region in July 2011.

2018). This would mean that surface NO_x emissions would likely be over diluted in the model. But this would be counter to the direction of the NO_x bias. Thus, while perhaps important for other emissions, it is likely not a factor in the present NO_x over-prediction. We also found CMAQ performed better on NO_x with finer grids, i.e., grid spacing of 4 km instead of 12 km (grey line in Fig. 3), particularly in coastal areas, indicating the mismatch between area represented by the grid-cell and the monitor location, which could also be responsible for the differences of NO_x between the model and observations.

3.2. The sensitivity simulations

3.2.1. MEGAN vs. BEIS

MEGAN simulated higher isoprene emissions than BEIS in the Great Lakes Region during July 2011. This was consistent with previous studies, e.g., isoprene emissions from MEGAN were approximately twice as high as BEIS emissions in Hogrefe et al. (2011), and a factor of two difference in VOC reactivity was found between MEGAN and BEIS in Carlton and Baker (2011). In this study, MEGAN isoprene emissions averaged across the domain in the daytime, i.e., 6:00–18:00 CST, are 50% higher than the BEIS emission (Fig. 5), with similar spatial variability— r^2 of ~0.8 for monthly mean and both showing high values over the southeastern part of the domain (BEIS emissions are shown in Fig. 5 (b)). However, MEGAN emissions were higher in isoprene-rich locations (the southeastern domain), and northeastern Minnesota, where the Superior National Forest is located, while BEIS emissions were not that high (Fig. 5 (c)). Higher emissions with MEGAN were caused by algorithmic differences from BEIS as discussed in Section 2.2.2.1, as well as using a different light response curve (Hogrefe et al., 2011). Evaluation of the biogenic emissions models suggested that simulated isoprene mixing ratio is higher with respect to measurements with MEGAN estimates (Bash et al., 2016; Carlton and Baker, 2011; Hogrefe et al., 2011; Kota et al., 2015).

Despite substantial changes in biogenic emissions with MEGAN, MDA8 O_3 presented little changes (± 1 ppb) over a large portion of the domain (Fig. 6). The small response of MDA8 O_3 to changes in biogenic emissions was consistent with other comparisons (Hogrefe et al., 2011; Zhang et al., 2017), and resulted from the NO_x-limited regime over most of the domain. The most notable enhancement of MDA8 O_3 over the lakes (1–2 ppb) and around Pittsburgh (up to 4–5 ppb) indicated that formation in these areas were likely VOC-limited as abundant NO_x transported from upwind directions (e.g., the southwestern coast of Lake Michigan) consumed OH radical and suppressed O_3 formation.

As a result of small increases in MDA8 O_3 along the shoreline of Lake Michigan, the positive biases of the simulations against observations became slightly larger (higher absolute mean biases), with an indication of worse performance (Fig. 7). On the other hand, biases for elevated MDA8 O_3 had little changes, i.e., ± 0.5 ppb in absolute biases at most sites along Lake Michigan, with better performance in a few locations. Improvements of simulated elevated MDA8 O_3 could also be found in the southeastern portion of the domain (Fig. 8). Using MEGAN did not appear to change model-observation agreement in terms of O_3 diurnal trends (green line in Fig. 3) as the simulation with MEGAN emissions were almost identical to the base case, regardless of the site category. On average, O_3 increased by 0.6 ppb at AQS sites within the modeling domain, which is minor compared to the monthly mean of ~50 ppb. Changed biogenic emissions also had a negligible influence on simulated NO_x concentration (not shown here) as biogenic NO_x was minor with respect to NO_x emissions of anthropogenic origin in the Great Lakes Region.

3.2.2. 50% reduction of NO_x emissions from on-road mobile sources

With 50% reduction of NO_x emissions from on-road mobile sources, MDA8 O_3 was lower than the base case over most areas of the domain by at least 1 ppb, with a maximum decrease of ~4 ppb in Ohio (Fig. 6). In city centers like Chicago, due to sufficient NO_x emissions from vehicles, MDA8 O_3 did not drop as significantly as in the surrounding areas, where O_3 formation was largely limited by the abundance of NO_x. MDA8 O_3 decreased by 1–3 ppb over the lakes.

Given that MDA8 O_3 is lower domain-wide than the base case, which showed high biases along the lakes, the performance improved near the shoreline with reduction of NO_x emissions (Fig. 7). However, in locations with low biases in the base case, e.g., in Michigan, the simulations became more biased with respect to the observations, corresponding to worse performance. This was also the case for elevated MDA8 O_3 (Fig. 8), the baseline of which was mostly lower than observations and decreased by 2–5 ppb further with reduction of NO_x emissions, though some improvements were also seen at coastal sites. By examining diurnal variations of O_3, it was seen that NO_x emissions from on-road mobile sources had a distinct impact on peak O_3 concentrations, particularly at sites more than 20 km away from the lake (containing more rural/suburban sites), bringing it down by ~4 ppb around noon and becoming closer to the observations. The high biases of O_3 at night and in the early morning (22:00–6:00 CST) were not sensitive to changes in NO_x emissions, implying that it could be caused by other issues, such as mixing in the model as discussed in Section 3.1, for example. On average, MDA8 O_3 decreased by ~2 ppb in inland areas, which could almost fill the gap between observations and simulations in the base case. However, only 1.4 ppb reduction of MDA8 O_3 occurred across the coastal areas, with high biases (~5 ppb) against

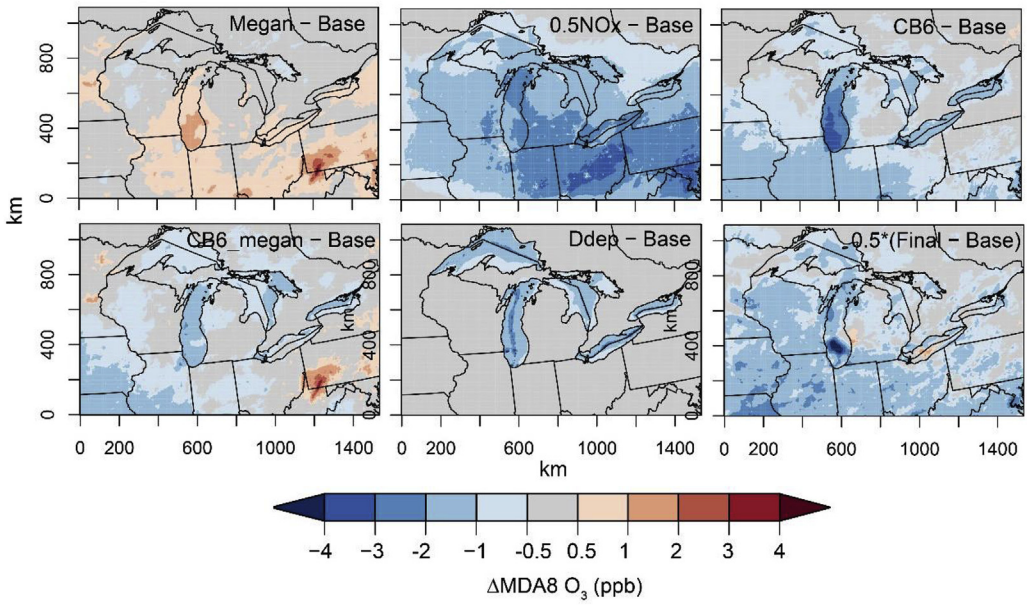

Fig. 6. Changes in MDA8 O_3 for each sensitivity run with respect to the base case over the Great Lakes Region in July 2011. Note that the lower right panel displays half of the changes in the final simulation.

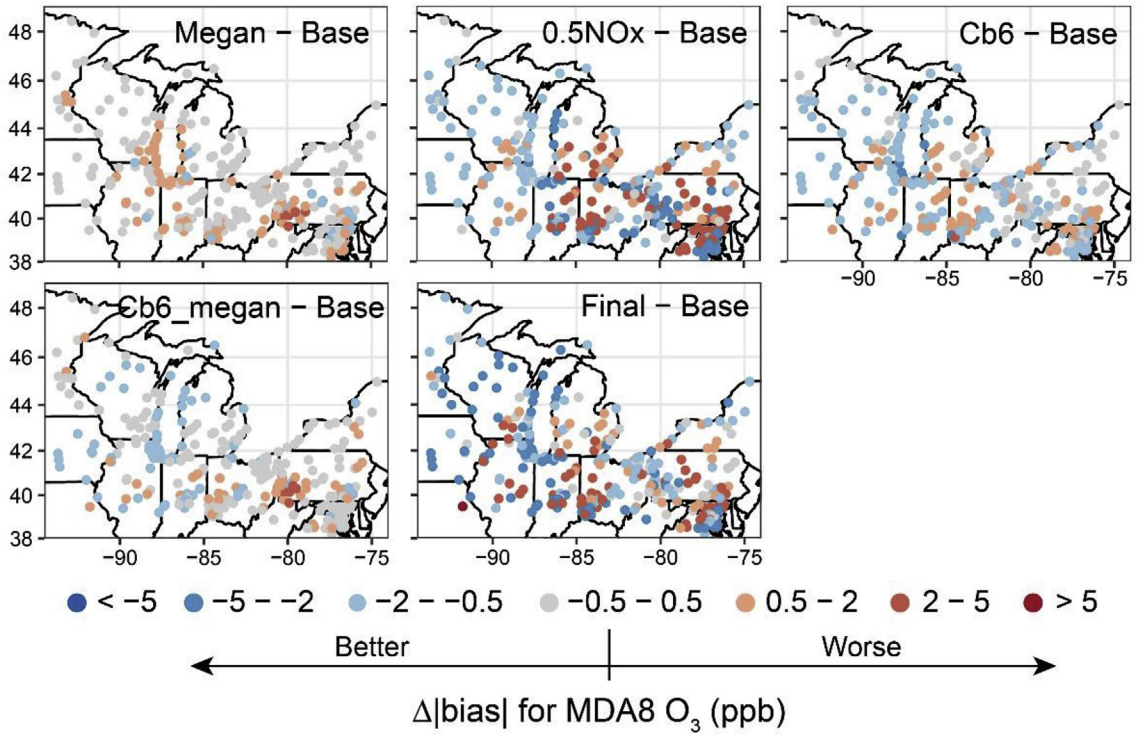

Fig. 7. Changes in absolute mean bias (MB) for MDA8 O_3 in each sensitivity run compared to the base case over the Great Lakes Region in July 2011, with negative values representing better performance than the base case and positive values representing worse performance.

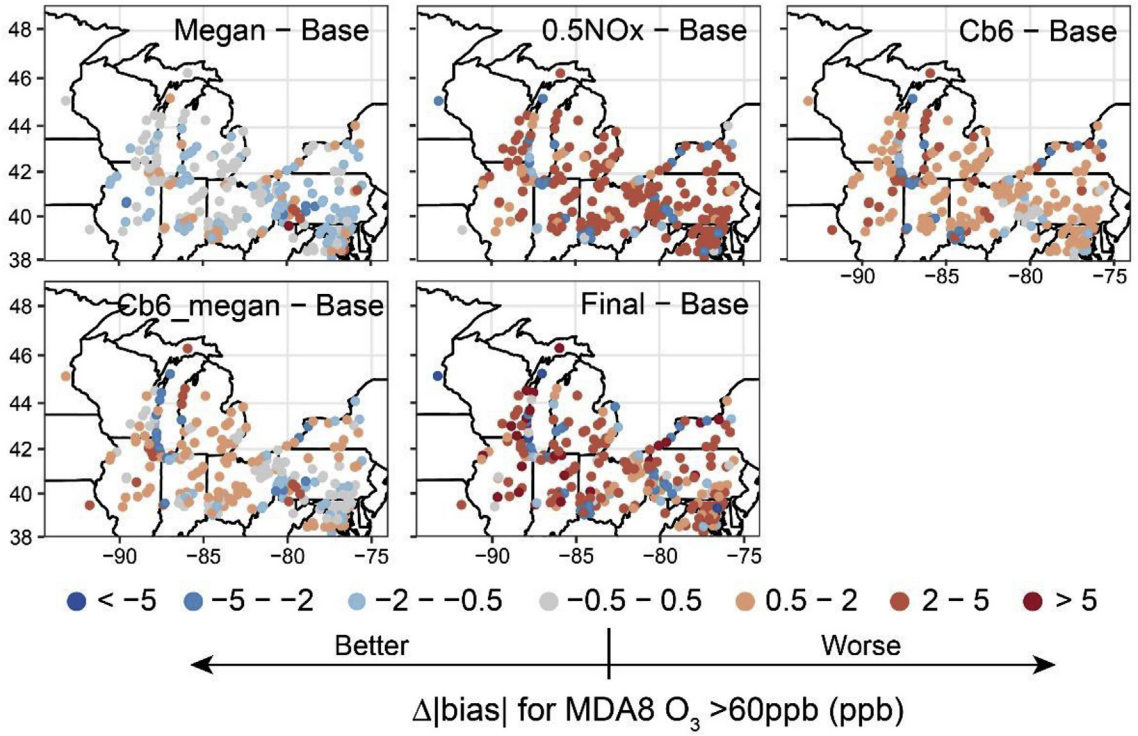

Fig. 8. Changes in absolute mean biases (MB) for elevated MDA8 O_3 (> 60 ppb) in each sensitivity run compared to the base case over the Great Lakes Region in July 2011, with negative values representing better performance than the base case and positive values representing worse performance.

observations remaining.

It was expected that reduction of NO_x emissions would result in better agreement of simulated NO_x concentrations with the observations, and this was true over the period from 22:00 to 7:00 CST (Fig. 3). Overestimates of NO_x were suppressed around morning rush-hour. According to our previous modeling by Odman et al. (2019a), inaccurate representation of land-water-interface could also lead to overestimates of NO_x in coastal areas where the model considers water and creates boundary layers that are too shallow. However, reducing NO_x emissions did not have any effect on high biases of NO_x in late

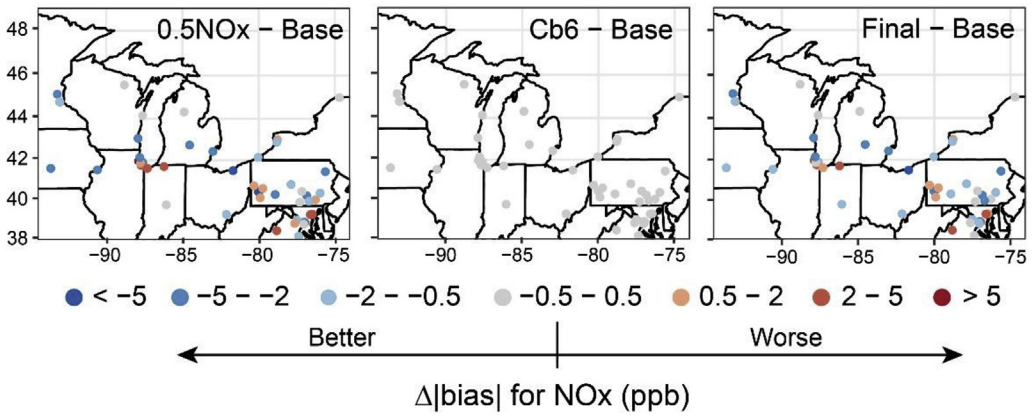

Fig. 9. Changes in absolute mean biases (MB) for NO_x in each sensitivity run compared to the base case over the Great Lakes Region in July 2011, with negative values representing better performance than the base case and positive values representing worse performance.

afternoon and early evening (17:00–21:00 CST) when nocturnal boundary layer begins to build. Another major issue with simulated NO_x was the underestimation during the daytime, and reduction of NO_x emissions could deteriorate the simulation over this period, particularly at coastal sites. This indicated that factors other than emissions, e.g., vertical mixing, inaccurate spatial/temporal allocation of mobile emissions, etc., which are under investigations (Henderson et al., 2017), could also be responsible for the biases in NO_x simulation. Further discussions on evaluations of NO_x emissions are beyond the scope of this study; however, more accurate representation of NO_x would likely lead to better performance on O_3.

Compared to the observations, model performance for NO_x in this sensitivity run was mostly improved in terms of monthly mean (Fig. 9), with ~14 ppb against the observed ~15 ppb for coastal areas, and ~8 ppb against ~9 ppb for inland sites (Fig. 3), which also suggested that a 50% reduction of NO_x emissions from on-road mobile sources might be more than what is necessary for better NO_x performance. By applying linear interpolation on the response of NO_x concentrations to changes in mobile emissions, we proposed that a 30% reduction of NO_x emissions from on-road mobile sources should be applied in the final simulation to best capture the observed NO_x concentrations, which agreed well with the 20–30% reduction recommended by McDonald et al. (2018).

3.2.3. CB6 vs. CB05

To test the impact of transition from CB05 to CB6, a newer version of CMAQ—CMAQv5.2 was used. Therefore, differences of simulated O_3 between the sensitivity run and the base case could be partly contributed by updates other than the chemical mechanism. However, based on incremental tests conducted by EPA (available at https://www.epa.gov/cmaq/incremental-evaluation-cmaqv52), the largest decrease in O_3 using CMAQv5.2 compared to CMAQv5.1 was attributed to the transition to CB6, rather than other O_3-related updates (e.g., increased O_3 deposition to wetted surfaces by scaling O_3 cuticular resistance, which is important in the early morning, and a reduction of the estimated cloud fractions with the updated sub-grid cloud scheme.) in CMAQv5.2. An accompanying error-correction of the dry deposition scheme slightly increased O_3 due to less dry deposition, which would cancel out most of the effect of the change in cuticular resistance. The effect of the update to the sub-grid cloud scheme was small compared to that of switching to CB6. As such, domain-wide lower MDA8 O_3 relative to the base case, with the differences reaching the maximum (~4 ppb) over southern Lake Michigan (Fig. 6), was primarily due to using a different chemical mechanism. Any of the multiple modifications with CB6 (CB6r3 in this study) could lead to changes in simulated O_3, such as revised NO_x recycling from organonitrates and removal of organonitrates within aerosols, and it is difficult to separate out individual effects.

For MDA8 O_3, changes in biases of the simulation with CB6 compared to the base case were mixed across the domain (Fig. 7). Generally, lower O_3 with CB6 had better agreement with observations, indicated by the blue colors along Lake Michigan and over the western domain. For sites with lower O_3 than observations in the base case, model-observation discrepancies became larger. The slight reductions of O_3 are consistent with the simulations for winter ozone (Emery et al., 2015; Matichuk et al., 2017). In the base case, CMAQ tended to underestimate elevated MDA8 O_3. The negative biases for elevated O_3 using CB6 were larger compared to the base case (Fig. 8), leading to worse performance on elevated O_3 with CB6. The impact of using CB6 was similar to that of reducing NO_x emissions, in terms of improvements/deteriorations for model comparison against the observations, with the effect of NO_x emissions reduction being more significant. However, O_3 decreased throughout the day using CB6 (Fig. 3), rather than just at peak concentration as seen with NO_x emissions reduction, although the changes were small. The case *CB6* simulated MDA8 O_3 0.6–1.2 ppb less than the base case, which was too small to cancel out high biases (1.8–6.3 ppb) in the base case. Based on the incremental tests mentioned above, CMAQv5.2 was able to lower NO_2 concentration compared to CMAQv5.1. However, we did not see a decrease of NO_x in our work.

The combination of CB6 with MEGAN emissions resulted in lower MDA8 O_3 (1–2 ppb) over the lakes, while O_3 on land was mostly unchanged compared to the base case (Fig. 6). The diurnal trends, in this case, resembled the base case as well. Only the coastal sites showed slight decreases (0.6 ppb) of monthly averaged MDA8 O_3 as a response to the combined changes in emissions and chemistry. Performance of MDA8 O_3 with or without a cutoff of 60 ppb both showed better consistency with observations along the shoreline of the lakes (Figs. 7 and 8), with larger low biases for elevated MDA8 O_3 in many locations across the domain.

3.2.4. Dry deposition

Tenfold increased dry deposition of O_3 over fresh water led to reductions of MDA8 O_3 of 0.5–2 ppb compared to the base case; however, this was restricted to over water (Fig. 6). The anomalous decrease of O_3 in the middle of the lakes was caused by an issue with the Spatial Allocator tool (available from ftp://ftp.epa.gov/EmisInventory/2011v6/v2platform/spatial_surrogates/) causing some grid cells representing the lakes to be mistakenly treated as sea water with much higher dry deposition velocity of O_3 than over fresh water in CMAQ. However, this problem can hardly affect simulated O_3 over land or at other grid cells representing water.

Changing dry deposition over water had a negligible impact on surface O_3, even in coastal regions (Fig. 10). Coastal O_3 dropped by up

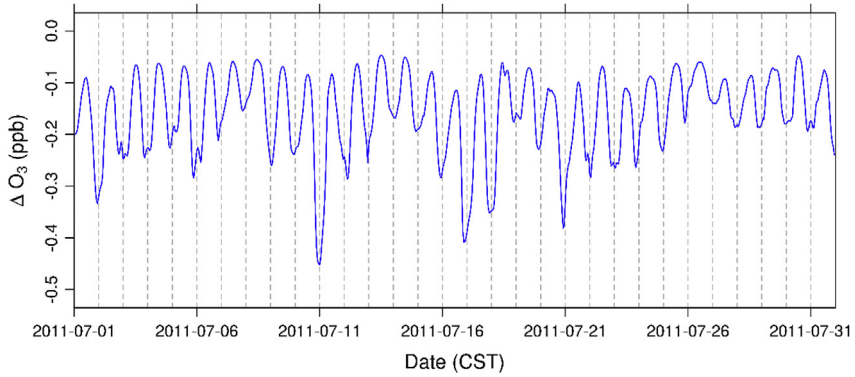

Fig. 10. Changes in O_3 concentration due to tenfold increased dry deposition velocity of O_3 over fresh water with respect to the base case in coastal areas over the Great Lakes Region in July 2011.

to ~0.5 ppb, with the largest decrease at night, which is in good agreement with the no-dry-deposition test conducted by Vieno et al. (2010). This was likely due to efficient O_3 production during the day time so that the influence of dry deposition was suppressed. The insensitivity of O_3 to dry deposition over fresh water can be explained by the insignificance of dry deposition of O_3 to water, which is controlled by surface resistance as O_3 is not soluble (Seinfeld and Pandis, 2012). High surface resistance for O_3 over water yields low dry deposition velocity; therefore, based on the results of this sensitivity case, dry deposition accounts for a small sink of O_3, and could not be responsible for the high biases of O_3 in the Great Lakes Region.

3.3. Final simulation

The final simulation was conducted as an attempt to achieve the best overall performance of O_3 and NO_x by using a combination of 30% reduction of NO_x emissions from on-road mobile sources, biogenic emissions with MEGAN, and CB6 chemical mechanism. According to the sensitivity runs, it was inferred that simulation of MDA8 O_3 could be improved significantly compared to the base case, while elevated MDA8 O_3 might become worse as the negative biases could be even lower across the domain, with an exception along Lake Michigan's shoreline, where elevated MDA8 O_3 was overestimated in the base case. However, neither the emissions/chemical mechanism used in the base case nor the alternatives in each sensitivity run could achieve better performance for both MDA8 O_3 and elevated MDA8 O_3. As a result, the approach used in the final run can be viewed as a tradeoff. One should note that the meteorology that drives the CMAQ final simulation also changed with a different nudging option, i.e., nudging above ~2 km instead of nudging above the planetary boundary layer (PBL), to avoid damping the amplitude of the nocturnal low level jet (Odman et al., 2019b).

The spatial variations of MDA8 O_3 across the domain in the final run were similar to the base case – higher O_3 over the lakes with the highest concentration near the southwestern coast of Lake Michigan (Fig. 11 (a)). There was a significant decrease of O_3, i.e., ~10 ppb over southern Lake Michigan, along with 4–6 ppb in a large part of the southern domain (Fig. 6). With lower simulated O_3 in the final run, the averaged concentrations at AQS sites in inland and buffer areas were quite close to the observations (mean biases near zero in Table 2), with NMB close to zero. Positive biases for MDA8 O_3 at coastal sites decreased as well, but the simulation remained ~5 ppb higher than observations, with a NMB of 9%. The spatial plot (Fig. 4) showed that overestimations of MDA8 O_3 were centered along the Lake Michigan shore. Comparing the absolute biases for MDA8 O_3 at every AQS site in the two cases (base and final) gave us an insight into whether the model performed better in the final run than the base case. It was found that 184 out of 291 sites within the domain had better performance in the final run, with lower absolute biases than in the base case (blue areas in Fig. 11 (b)), and this was mainly due to the decreased high biases at most sites. The improvements were mostly found along the lakeshores and in the western Great Lakes Region (Fig. 7). A recent paper gave an alternative hypothesis for the common positive biases for surface O_3 in multiple air quality models, i.e., the lack of photolysis reduction associated with foliage and the turbulence reductions due to forest canopies (Makar et al., 2017). This could not explain the significant high biases of O_3 along the shoreline in our case; however, it is worth being investigated in future work, particularly in densely forested areas.

As expected, the final simulation produced lower elevated MDA8 O_3 (> 60 ppb) than the base case. This resulted in simulations, which were originally biased low, becoming more biased with respect to the observations (Fig. 11 (c)). However, performance improved at some sites along the coast, in southwestern Ohio, and in Pennsylvania (Fig. 8), which accounted for 24% of all AQS sites across the domain. Elevated MDA8 O_3 was biased low by 3–9 ppb in the final run, with NMB ranging from −4 to −13%, as compared to the base case with MB of 0 to −6 ppb and NMB of 0 to −8%. Diurnal trends of O_3 in the final simulation showed that the decrease tended to occur between 10:00–17:00 CST, which was very similar to that in the case *0.5NO$_x$*, indicating that reduction of NO_x emissions had a major effect on simulated O_3 over land.

With 30% reduction of NO_x emissions from on-road mobile sources, simulated NO_x was ~14 ppb at coastal sites compared to the observed ~15 ppb, and ~9 ppb in inland areas, which was almost unbiased from the observations (Fig. 3). Similar to the case *0.5NO$_x$*, high biases of NO_x in the early evening still existed and daytime NO_x was biased low. Overall, 60% of the sites, most of which were located in the south of the domain, had better simulation performance for NO_x than the base case (Fig. 9).

3.4. Impact of lateral boundary conditions (LBCs)

One uncertainty in the simulations is that predefined default LBCs applied in CMAQ simulations for the outer domain could bias the results. An additional simulation over the 12-km domain was conducted, using LBCs that had been extracted from a GEOS-Chem simulation for July 2011, with other inputs or configurations being the same as the final run. Using the LBCs from GEOS-Chem leads to lower MDA8 O_3 near the western boundary of the 12-km domain (Fig. 12 (a)). In contrast, MDA8 O_3 is higher across most of the continental US, particularly in the high-elevation region of the intermountain west, which is driven by higher LBCs of O_3 aloft (above ~4 km) from GEOS-Chem (Fig. S2). Compared to other regions across the US, the Midwest is less impacted by LBCs for the outer domain (the changes in simulated MDA8 O_3 are in the range of ± 2 ppb).

An examination of vertical distribution of O_3 in LBCs at the western

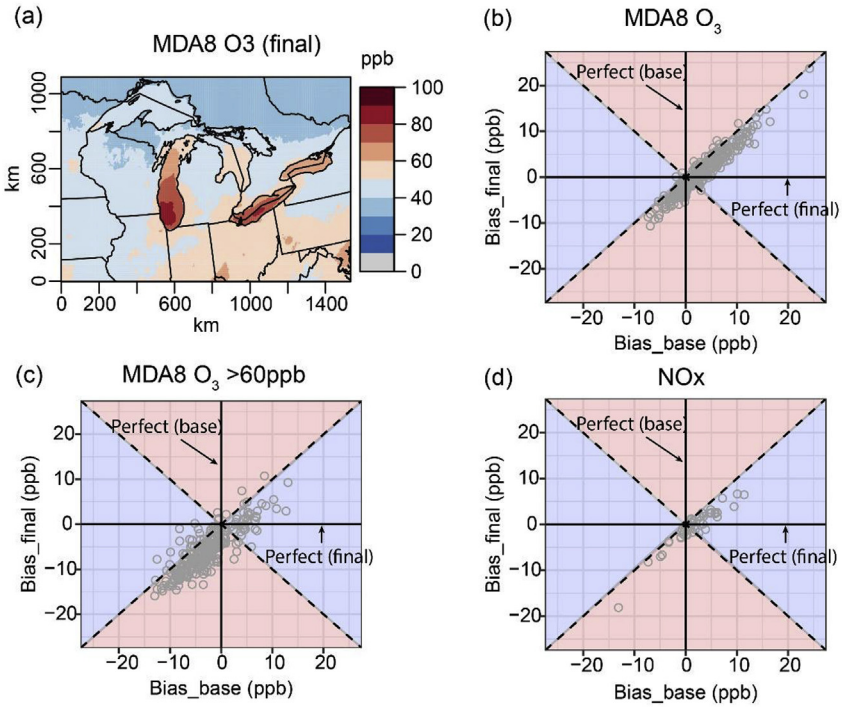

Fig. 11. (a) Simulated MDA8 O_3 in the final simulation over the Great Lakes Region in July 2011. (b) Scatter plot of biases for MDA8 O_3 in the final simulation against biases for MDA8 O_3 in the base case at the AQS sites. (c) Scatter plot of biases for elevated MDA8 O_3 in the final simulation against biases of elevated MDA8 O_3 in the base case at the AQS sites. (d) Scatter plot of biases for NO_x in the final simulation against biases of NO_x in the base case at the AQS sites. The x axis and y axis in the scatter plots represents perfect performance (bias of zero against observations) for the final simulation and base case, respectively. The blue areas represent that the final simulation performed better than the base case, with the red areas showing the opposite. (For interpretation of the references to color in this figure legend, the reader is referred to the Web version of this article.)

and southern boundary for the 4-km domain showed that they are almost identical below 2 km, with significant differences in the middle to upper troposphere and stratosphere (Fig. 12 (b)). We do not expect this to influence the surface O_3 within the inner domain substantially, unless deep convective mixing or stratospheric intrusion occurs. On the other hand, the total contributions of LBCs to surface O_3 could be less due to efficient formation of O_3 regionally in summer (Baker et al., 2015). While the impact of LBCs for the outer domain is insignificant in our 4-km resolution Great Lakes Region simulation, this might not be the case in a different location or season, or at continental scales (Astitha et al., 2018; Hogrefe et al., 2018; Im et al., 2018; Mathur et al., 2017). Besides, using predefined O_3 profiles in CMAQ could lead to significantly lower O_3 in the middle to upper troposphere, as revealed by a comparison of the CMAQ simulation in this work with O_3 observations from the ozonesonde at Egbert, Canada (Fig. S3). Therefore, we recommend using LBCs from global chemical transport models.

4. Conclusions

This study applied the CMAQ model to simulate surface O_3 over the Great Lakes Region in July 2011 at a resolution of 4 km, and evaluated model performance using ground-based observations at the AQS sites. The model simulated elevated MDA8 O_3 over the lakes, with the highest level (> 90 ppb) simulated to the southwestern side of Lake Michigan. Coastal O_3 was biased high, by ~6 ppb on average, and O_3 at inland sites (100 km further away from the shoreline) was ~2 ppb higher than

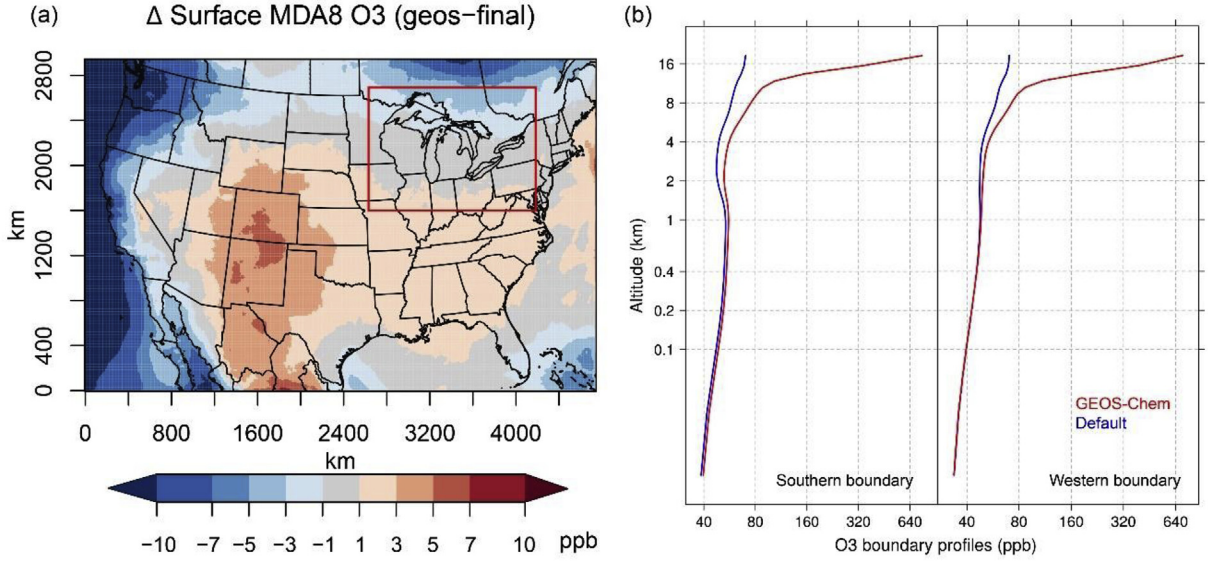

Fig. 12. (a) Changes in simulated MDA8 O_3 (ppb) using lateral boundary conditions (LBCs) from GEOS-Chem instead of the predefined profiles in CMAQ for the outer domain during July 2011. The inner domain is indicated with the red box. (b) O_3 LBCs at the southern and western boundary for the inner domain, derived from 12-km simulations using LBCs from GEOS-Chem (red) and the predefined profiles (blue) in CMAQ, respectively. (For interpretation of the references to color in this figure legend, the reader is referred to the Web version of this article.)

the observations. High biases were more significant during the early mornings (0:00–5:00 CST) and over periods when O_3 was accumulating (8:00–16:00 CST). However, elevated MDA8 O_3 (> 60 ppb) was biased low throughout the domain, with exceptions centered along the Lake Michigan shore. As such, five sensitivity runs were conducted with: 1) different biogenic emissions by using MEGAN instead of BEIS; 2) 50% reduction of NO_x emissions from on-road mobile sources; 3) different chemical mechanism (i.e., CB6 instead of CB05); 4) a combination of MEGAN biogenic emissions and CB6 chemical mechanism instead of BEIS emissions and CB05; and, 5) enhanced dry deposition velocity of O_3 over fresh water; to examine the role of emissions, chemistry and deposition in the overestimation of O_3 in this region.

Despite 50% higher isoprene emissions in the daytime with MEGAN compared to BEIS across the domain, simulated MDA8 O_3 with MEGAN emissions changed very little from the base case over a large portion of the domain, with the most notable enhancement over the lake (1–2 ppb) and around Pittsburgh, Pennsylvania (up to 4–5 ppb). As a result, using MEGAN did not improve model performance on MDA8 O_3, while elevated MDA8 O_3 was slightly better than the base case in the southeastern domain. Changing O_3 dry deposition to fresh water had a negligible effect on simulated O_3 as well. Increasing dry deposition of O_3 over water by a factor of 10 decreased MDA8 O_3 by no more than 2 ppb over water, and hardly affected O_3 concentrations over land.

Both the 50% reduction of NO_x emissions from on-road mobile sources and using CB6 instead of CB05 led to domain-wide lower MDA8 O_3 than the base case. The largest decrease with CB6 (~4 ppb) was over Lake Michigan, with smaller changes over land (< 2 ppb); adjustment of NO_x emissions decreased MDA8 O_3 by 2–4 ppb over the southeastern domain and less in urban areas. Improved performance on MDA8 O_3 in these two sensitivity runs were concentrated in coastal areas and the western domain, where O_3 was mostly biased high in the base case. Elevated MDA8 O_3 was more biased than in the base case (except along the coast of Lake Michigan) as the original low values now became even lower. Reduction of NO_x emissions made the simulated daily peak O_3 closer to the observation and suppressed the high biases of NO_x around 6:00 CST. The combination of MEGAN and CB6 had slightly better performance on O_3 along the lakeshores, with noticeable improvements of elevated MDA8 O_3 along the western coast of Lake Michigan.

Based on the sensitivity tests, we recommend a 30% reduction of NO_x emissions from on-road mobile sources if the 2011 NEI is used to represent anthropogenic emissions, as well as the use of CB6 mechanism to simulate domain-wide lower MDA8 O_3 and decrease the high biases across the domain. MEGAN was chosen to estimate biogenic emissions because better performance on elevated MDA8 O_3 could be obtained in the coastal areas. The final simulations with these recommendations resulted in substantial decreases of MDA8 O_3, i.e., ~10 ppb over Lake Michigan and 4–6 ppb in the southern domain. Model performance significantly improved compared to the base case at most (~60%) AQS sites, and this was particularly the case along Lake Michigan shoreline. Low biases for elevated O_3 over a large part of the domain were larger in the final run, however, slightly better performance than in the base case was found along Lake Michigan. Additionally, high biases for peak O_3 during the daytime were also suppressed in inland/buffer areas primarily due to the adjustment of NO_x emissions.

This study provides a set of choices for chemical mechanism, deposition rate, and emissions to optimize O_3 simulations in the Great Lakes Region with the CMAQ model. It is important to note that the recommended choices pertain to 2011, assuming that 2011 NEI is used. Besides, there are still issues with the simulations to be addressed in the future; for instance, high biases along the lakeshores remained and MDA8 O_3 larger than 60 ppb was biased low across the domain except at coastal areas. O_3 simulation performance over water could be affecting model performance along the shoreline; however, measurements offshore, such as ferry-based measurements available for model evaluation, are too limited to perform an evaluation. O_3 vertical distributions would also be helpful to better understand the causes for model overestimation and a comparison is warranted once such measurements in the Great Lakes Region become available. Given that biogenic emissions have a significant impact on simulated MDA8 O_3 while evaluation of MDA8 O_3 cannot reveal which emission model is better, biogenic VOC measurements would be extremely useful for this region so that a more informed choice of emission model could be made in the future.

Declaration of interests

The authors declare the following financial interests/personal relationships which may be considered as potential competing interests: We declared that co-author Eladio Knipping is employed by the Electric Power Research Institute, which is one of the organizations funding this research.

Acknowledgements

We are grateful to three anonymous reviewers and Dr. James Schauer for their constructive comments that helped us significantly improve the manuscript. We would like to thank Dr. Rohit Mathur for helpful discussions on the impact of lateral boundary conditions, and Dr. Tao Zeng for providing us with the GEOS-Chem simulations. We appreciate the help from Gertrude K. Pavur for language editing. This research was funded by the Electric Power Research Institute grant number 10005953 and the National Aeronautics and Space Administration Applied Sciences Program grant number NNX16AQ29G. The contents of the publication are solely the responsibility of the grantee and do not necessarily represent the official views of the supporting agencies. Further, The USA Government does not endorse the purchase of any commercial products or services mentioned in the publication.

Appendix A. Supplementary data

Supplementary data to this article can be found online at https://doi.org/10.1016/j.atmosenv.2019.01.025.

References

Anderson, D.C., Loughner, C.P., Diskin, G., Weinheimer, A., Canty, T.P., Salawitch, R.J., Worden, H.M., Fried, A., Mikoviny, T., Wisthaler, A., 2014. Measured and modeled CO and NOy in DISCOVER-AQ: an evaluation of emissions and chemistry over the eastern US. Atmos. Environ. 96, 78–87.

Astitha, M., Kioutsoukis, I., Fisseha, G.A., Bianconi, R., Bieser, J., Christensen, J.H., Cooper, O., Galmarini, S., Hogrefe, C., Im, U., Johnson, B., Liu, P., Nopmongcol, U., Petropavlovskikh, I., Solazzo, E., Tarasick, D.W., Yarwood, G., 2018. Seasonal ozone vertical profiles over North America using the AQMEII group of air quality models: model inter-comparison and stratospheric intrusions. Atmos. Chem. Phys. 18, 13925–13945.

Baker, K.R., Emery, C., Dolwick, P., Yarwood, G., 2015. Photochemical grid model estimates of lateral boundary contributions to ozone and particulate matter across the continental United States. Atmos. Environ. 123, 49–62.

Bash, J.O., Baker, K.R., Beaver, M.R., 2016. Evaluation of improved land use and canopy representation in BEIS v3. 61 with biogenic VOC measurements in California. Geosci. Model Dev. (GMD) 9, 2191.

Bosveld, F.C., Baas, P., Steeneveld, G.-J., Holtslag, A.A., Angevine, W.M., Bazile, E., de Bruijn, E.I., Deacu, D., Edwards, J.M., Ek, M., 2014. The third GABLS intercomparison case for evaluation studies of boundary-layer models. Part B: results and process understanding. Boundary-Layer Meteorol. 152, 157–187.

Byun, D., Schere, K.L., 2006. Review of the governing equations, computational algorithms, and other components of the Models-3 Community Multiscale Air Quality (CMAQ) modeling system. Appl. Mech. Rev. 59, 51–77.

Canty, T., Hembeck, L., Vinciguerra, T., Goldberg, D., Carpenter, S., Allen, D., Loughner, C., Salawitch, R., Dickerson, R., 2015. Ozone and NOx chemistry in the eastern US: evaluation of CMAQ/CB05 with satellite (OMI) data. Atmos. Chem. Phys. 15, 10965.

Carlton, A.G., Baker, K.R., 2011. Photochemical modeling of the Ozark isoprene volcano: MEGAN, BEIS, and their impacts on air quality predictions. Environ. Sci. Technol. 45, 4438–4445.

Cleary, P., Fuhrman, N., Schulz, L., Schafer, J., Fillingham, J., Bootsma, H., McQueen, J., Tang, Y., Langel, T., McKeen, S., 2015. Ozone distributions over southern Lake Michigan: comparisons between ferry-based observations, shoreline-based DOAS observations and model forecasts. Atmos. Chem. Phys. 15, 5109–5122.

Dye, T.S., Roberts, P.T., Korc, M.E., 1995. Observations of transport processes for ozone

and ozone precursors during the 1991 Lake Michigan Ozone Study. J. Appl. Meteorol. 34, 1877–1889.
Emery, C., Jung, J., Koo, B., Yarwood, G., 2015. Improvements to CAMx snow cover treatments and Carbon Bond chemical mechanism for winter ozone. UDAQ PO 480 52000000001.
Emery, C., Liu, Z., Russell, A.G., Odman, M.T., Yarwood, G., Kumar, N., 2017. Recommendations on statistics and benchmarks to assess photochemical model performance. J. Air Waste Manag. Assoc. 67, 582–598.
Fahey, K.M., Carlton, A.G., Pye, H.O., Baek, J., Hutzell, W.T., Stanier, C.O., Baker, K.R., Appel, K.W., Jaoui, M., Offenberg, J.H., 2017. A framework for expanding aqueous chemistry in the Community Multiscale Air Quality (CMAQ) model version 5.1. Geosci. Model Dev. (GMD) 10, 1587.
Fast, J.D., Heilman, W.E., 2003. The effect of lake temperatures and emissions on ozone exposure in the western Great Lakes region. J. Appl. Meteorol. 42, 1197–1217.
Foley, T., Betterton, E.A., Jacko, P.R., Hillery, J., 2011. Lake Michigan air quality: the 1994–2003 LADCO aircraft Project (LAP). Atmos. Environ. 45, 3192–3202.
Gipson, G.L., 1999. The Initial Concentration and Boundary Condition Processors. Science Algorithms of the EPA Models-3 Community Multiscale Air Quality (CMAQ) Modeling System. EPA-600/R-99/030. US Environmental Protection Agency, Research Triangle Park, NC.
Guenther, A., Jiang, X., Heald, C., Sakulyanontvittaya, T., Duhl, T., Emmons, L., Wang, X., 2012. The Model of Emissions of Gases and Aerosols from Nature Version 2.1 (MEGAN2. 1): an Extended and Updated Framework for Modeling Biogenic Emissions.
Hanna, S.R., Moore, G.E., Fernau, M.E., 1996. Evaluation of photochemical grid models (UAM-IV, UAM-V, and the ROM/UAM-IV couple) using data from the Lake Michigan Ozone Study (LMOS). Atmos. Environ. 30, 3265–3279.
Henderson, B., Simon, H., Timin, B., Dolwick, P., Owen, R., Eyth, A., Foley, K., Toro, C., Baker, K., Beardsley, M., Appel, K., McDonald, B., 2017. Evaluation of NOx Emissions and Modeling, 2017 CMAS Conference. Chapel Hill, NC.
Hildebrandt Ruiz, L., Yarwood, G., 2013. Interactions between Organic Aerosol and NOy: Influence on Oxidant Production, Final Report for AQRP Project 12-012. Prepared for the Texas Air Quality Research Program.
Hogrefe, C., Isukapalli, S.S., Tang, X., Georgopoulos, P.G., He, S., Zalewsky, E.E., Hao, W., Ku, J.-Y., Key, T., Sistla, G., 2011. Impact of biogenic emission uncertainties on the simulated response of ozone and fine particulate matter to anthropogenic emission reductions. J. Air Waste Manag. Assoc. 61, 92–108.
Hogrefe, C., Liu, P., Pouliot, G., Mathur, R., Roselle, S., Flemming, J., Lin, M., Park, R.J., 2018. Impacts of different characterizations of large-scale background on simulated regional-scale ozone over the continental United States. Atmos. Chem. Phys. 18.
Im, U., Christensen, J.H., Geels, C., Hansen, K.M., Brandt, J., Solazzo, E., Alyuz, U., Balzarini, A., Baro, R., Bellasio, R., 2018. Influence of anthropogenic emissions and boundary conditions on multi-model simulations of major air pollutants over Europe and North America in the framework of AQMEII3. Atmos. Chem. Phys. 18, 8929–8952.
Kota, S.H., Schade, G., Estes, M., Boyer, D., Ying, Q., 2015. Evaluation of MEGAN predicted biogenic isoprene emissions at urban locations in Southeast Texas. Atmos. Environ. 110, 54–64.
Lelieveld, J., Dentener, F.J., 2000. What controls tropospheric ozone? J. Geophys. Res.: Atmosphere 105, 3531–3551.
Lennartson, G.J., Schwartz, M.D., 2002. The lake breeze–ground-level ozone connection in eastern Wisconsin: a climatological perspective. Int. J. Climatol. 22, 1347–1364.
Levy, I., Makar, P., Sills, D., Zhang, J., Hayden, K., Mihele, C., Narayan, J., Moran, M., Sjostedt, S., Brook, J., 2010. Unraveling the complex local-scale flows influencing ozone patterns in the southern Great Lakes of North America. Atmos. Chem. Phys. 10, 10895–10915.
Li, J., Mao, J., Min, K.E., Washenfelder, R.A., Brown, S.S., Kaiser, J., Keutsch, F.N., Volkamer, R., Wolfe, G.M., Hanisco, T.F., 2016. Observational constraints on glyoxal production from isoprene oxidation and its contribution to organic aerosol over the Southeast United States. J. Geophys. Res.: Atmosphere 121, 9849–9861.
Lin, J.-T., Youn, D., Liang, X.-Z., Wuebbles, D.J., 2008. Global model simulation of summertime US ozone diurnal cycle and its sensitivity to PBL mixing, spatial resolution, and emissions. Atmos. Environ. 42, 8470–8483.
Makar, P., Gong, W., Mooney, C., Zhang, J., Davignon, D., Samaali, M., Moran, M., He, H., Tarasick, D., Sills, D., 2010a. Dynamic adjustment of climatological ozone boundary conditions for air-quality forecasts. Atmos. Chem. Phys. 10, 8997–9015.
Makar, P., Staebler, R., Akingunola, A., Zhang, J., McLinden, C., Kharol, S., Pabla, B., Cheung, P., Zheng, Q., 2017. The effects of forest canopy shading and turbulence on boundary layer ozone. Nat. Commun. 8, 15243.
Makar, P., Zhang, J., Gong, W., Stroud, C., Sills, D., Hayden, K., Brook, J., Levy, I., Mihele, C., Moran, M., 2010b. Mass tracking for chemical analysis: the causes of ozone formation in southern Ontario during BAQS-Met 2007. Atmos. Chem. Phys. 10, 11151.
Mathur, R., Xing, J., Gilliam, R., Sarwar, G., Hogrefe, C., Pleim, J., Pouliot, G., Roselle, S., Spero, T.L., Wong, D.C., 2017. Extending the Community Multiscale Air Quality (CMAQ) modeling system to hemispheric scales: overview of process considerations and initial applications. Atmos. Chem. Phys. 17, 12449.
Matichuk, R., Tonnesen, G., Luecken, D., Gilliam, R., Napelenok, S.L., Baker, K.R., Schwede, D., Murphy, B., Helmig, D., Lyman, S.N., 2017. Evaluation of the community Multiscale Air quality model for simulating winter ozone formation in the uinta basin. J. Geophys. Res.: Atmosphere 122 (13) 545-513,572.
McDonald, B., McKeen, S., Cui, Y.Y., Ahmadov, R., Kim, S.-W., Frost, G.J., Pollack, I., Peischl, J., Ryerson, T.B., Holloway, J., 2018. Modeling ozone in the eastern US using a fuel-based mobile source emissions inventory. Environ. Sci. Technol. 52, 7360–7370.
McNider, R.T., Pour-Biazar, A., Doty, K., White, A., Wu, Y., Qin, M., Hu, Y., Odman, M.T., Cleary, P., Knipping, E., Dornblaser, B., Lee, P., Hain, C., Mckeen, S., 2018. Examination of the physical atmosphere in the Great lakes region and its potential impact on air quality— overwater stability and satellite assimilation. Journal of Applied Meteorology and Climatology 57, 2789–2816.
Odman, M.T., Qin, M., Hu, Y., Russell, A.G., Boylan, J.W., 2019a. 2017 projections and interstate transport of ozone in the southeastern United States. J. Environ. Manag (submitted).
Odman, M.T., White, A.T., Doty, K., McNider, R.T., Pour-Biazar, A., Qin, M., Hu, Y., Knipping, E., Wu, Y., Dornblaser, B., 2019b. Examination of the physical atmosphere in the Great lakes region and its potential impact on air quality: FDDA strategies. Journal of Applied Meteorology and Climatology (revisions submitted).
Park, R., Hong, S.K., Kwon, H.-A., Kim, S., Guenther, A., Woo, J.-H., Loughner, C., 2014. An evaluation of ozone dry deposition simulations in East Asia. Atmos. Chem. Phys. 14, 7929–7940.
Pleim, J.E., Gilliam, R., 2009. An indirect data assimilation scheme for deep soil temperature in the Pleim–Xiu land surface model. Journal of Applied Meteorology and Climatology 48, 1362–1376.
Pleim, J.E., Xiu, A., 2003. Development of a land surface model. Part II: data assimilation. J. Appl. Meteorol. 42, 1811–1822.
Pouliot, G., Pierce, T., 2009. Integration of the model of emissions of Gases and aerosols from nature (MEGAN) into the CMAQ modeling system. In: 18th International Emission Inventory Conference, Baltimore, Maryland, pp. 14–17.
Pour Biazar, A., McNider, R.T., Doty, K., White, A., Wu, Y., Qin, M., Hu, Y., Odman, M.T., Dornblaser, B., Cleary, P., Knipping, E., McKeen, S., Lee, P., 2018. In: Multiyear Model Evaluation over Lake Michigan Region. 2018 CMAS Conference. Chapel Hill, NC.
Pugliese, S., Murphy, J., Geddes, J., Wang, J., 2014. The impacts of precursor reduction and meteorology on ground-level ozone in the Greater Toronto Area. Atmos. Chem. Phys. 14, 8197–8207.
Sarwar, G., Gantt, B., Schwede, D., Foley, K., Mathur, R., Saiz-Lopez, A., 2015. Impact of enhanced ozone deposition and halogen chemistry on tropospheric ozone over the Northern Hemisphere. Environ. Sci. Technol. 49, 9203–9211.
Savijärvi, H., 2009. Stable boundary layer: parametrizations for local and larger scales. Q. J. R. Meteorol. Soc. 135, 914–921.
Seinfeld, J.H., Pandis, S.N., 2012. Atmospheric Chemistry and Physics: from Air Pollution to Climate Change.
Sills, D., Brook, J., Levy, I., Makar, P., Zhang, J., Taylor, P., 2011. Lake breezes in the southern Great Lakes region and their influence during BAQS-Met 2007. Atmos. Chem. Phys. 11, 7955–7973.
Simon, H., Baker, K.R., Phillips, S., 2012. Compilation and interpretation of photochemical model performance statistics published between 2006 and 2012. Atmos. Environ. 61, 124–139.
Simon, H., Valin, L.C., Baker, K.R., Henderson, B.H., Crawford, J.H., Pusede, S.E., Kelly, J.T., Foley, K.M., Owen, R.C., Cohen, R.C., 2018. Characterizing CO and NOy sources and relative ambient ratios in the baltimore area using ambient measurements and source attribution modeling. J. Geophys. Res.: Atmosphere 123, 3304–3320.
Sindelarova, K., Granier, C., Bouarar, I., Guenther, A., Tilmes, S., Stavrakou, T., Müller, J.-F., Kuhn, U., Stefani, P., Knorr, W., 2014. Global data set of biogenic VOC emissions calculated by the MEGAN model over the last 30 years. Atmos. Chem. Phys. 14, 9317–9341.
Skamarock, W.C., Klemp, J.B., Dudhia, J., Gill, D.O., Barker, D.M., Wang, W., Powers, J.G., 2005. A Description of the Advanced Research WRF Version 2. National Center for Atmospheric Research Boulder Co Mesoscale and Microscale Meteorology Div.
Souri, A.H., Choi, Y., Jeon, W., Li, X., Pan, S., Diao, L., Westenbarger, D.A., 2016. Constraining NOx emissions using satellite NO2 measurements during 2013 DISCOVER-AQ Texas campaign. Atmos. Environ. 131, 371–381.
Stanier, C., Abdioskouei, M., Carmichael, G., Christiansen, M., Sobhani, N., 2017. Meteorological Air Quality Forecasting Using the WRF-Chem Model during the LMOS2017 Field Campaign. AGU Fall Meeting Abstracts.
Stoeckenius, T., McNally, D., 2014. Final Report 2013 Unita Basin Winter Ozone Study. ENVIRON International Corporation, Novato, California.
Travis, K.R., Jacob, D.J., Fisher, J.A., Kim, P.S., Marais, E.A., Zhu, L., Yu, K., Miller, C.C., Yantosca, R.M., Sulprizio, M.P., 2016. Why do models overestimate surface ozone in the Southeast United States? Atmos. Chem. Phys. 16, 13561–13577.
United States Environmental Protection Agency (US EPA), 2018. National Map of Ozone (2008) Nonattainment Areas. https://www3.epa.gov/airquality/greenbook/map8hr_2008.html.
Vieno, M., Dore, A., Stevenson, D.S., Doherty, R., Heal, M.R., Reis, S., Hallsworth, S., Tarrason, L., Wind, P., Fowler, D., 2010. Modelling surface ozone during the 2003 heat-wave in the UK. Atmos. Chem. Phys. 10, 7963–7978.
Wentworth, G., Murphy, J., Sills, D., 2015. Impact of lake breezes on ozone and nitrogen oxides in the Greater Toronto Area. Atmos. Environ. 109, 52–60.
Wesely, M., 1989. Parameterization of surface resistances to gaseous dry deposition in regional-scale numerical models. Atmos. Environ. 23 (1967), 1293–1304.
Wyat Appel, K., Napelenok, S., Hogrefe, C., Pouliot, G., Foley, K.M., Roselle, S.J., Pleim, J.E., Bash, J., Pye, H.O.T., Heath, N., Murphy, B., Mathur, R., 2018. Overview and Evaluation of the Community Multiscale Air Quality (CMAQ) Modeling System Version 5.2. Springer International Publishing, Cham, pp. 69–73.
Yarwood, G., Heo, G., Carter, W., Whitten, G., 2012. Environmental Chamber Experiments to Evaluate NOx Sinks and Recycling in Atmospheric Chemical Mechanisms. Final Report, Prepared for Dr. Elena C. McDonald-Buller, Texas Air Quality Research Program. The University of Texas at Austin, AQRP Project, pp. 10–042.
Yarwood, G., Jung, J., Whitten, G.Z., Heo, G., Mellberg, J., Estes, M., 2010. Updates to the Carbon Bond Mechanism for Version 6 (CB6), 2010 CMAS Conference. Chapel Hill, NC. October. http://www.cmascenter.org/conference/2010/abstracts/emery_updates_carbon_2010.pdf.
Yu, H., Guenther, A., Gu, D., Warneke, C., Geron, C., Goldstein, A., Graus, M., Karl, T., Kaser, L., Misztal, P., 2017. Airborne measurements of isoprene and monoterpene emissions from southeastern US forests. Sci. Total Environ. 595, 149–158.
Zhang, R., Cohan, A., Biazar, A.P., Cohan, D.S., 2017. Source apportionment of biogenic contributions to ozone formation over the United States. Atmos. Environ. 164, 8–19.